NASA Technical Memorandum 106504

Stagnation Region Heat Transfer: The Influence of Turbulence Parameters, Reynolds Number and Body Shape

G. James Van Fossen and Robert J. Simoneau
Lewis Research Center
Cleveland, Ohio

Prepared for the
Sixth AIAA/ASME Thermophysics and Heat Transfer Conference
cosponsored by the American Institute of Aeronautics and Astronautics and the
American Society of Mechanical Engineers
Colorado Springs, Colorado, June 20–23, 1994

NASA

STAGNATION REGION HEAT TRANSFER: THE INFLUENCE OF TURBULENCE PARAMETERS, REYNOLDS NUMBER AND BODY SHAPE

G. James Van Fossen

Robert J. Simoneau

Internal Fluid Mechanics Division
NASA Lewis Research Center
Cleveland, Ohio

ABSTRACT

The effect of velocity gradient on stagnation region heat transfer augmentation by free stream turbulence was investigated. Heat transfer was measured in the stagnation region of four models with elliptical leading edges with ratios of major to minor axes of 1:1, 1.5:1, 2.25:1, and 3:1. Four geometrically similar, square bar, square mesh, biplane grids were used to generate free stream turbulence with different intensities and length scales. Heat transfer measurements were made for the following ranges of parameters: Reynolds number, based on leading edge diameter, 37,000 to 228,000; dimensionless leading edge velocity gradient, 1.20 to 1.80; turbulence intensity, 1.1 to 15.9%; and length scale to leading edge diameter ratio, 0.05 to 0.30. Stagnation point heat transfer augmentation by free stream turbulence can be predicted using a modified version of a previously developed correlation for a circular leading edge. Heat transfer augmentation was independent of body shape at the stagnation point. The heat transfer distribution downstream from the stagnation point can be predicted using the normalized laminar heat transfer distribution.

INTRODUCTION

The heat transfer distribution around a streamlined object immersed in a flow usually has a maximum in the stagnation region. Cooling the stagnation region is important in many industrial application; however, none is more critical than in the modern high efficiency gas turbine. Combustor exit temperatures often exceed the melting temperature of superalloy turbine vane materials. Accurate prediction of stagnation region heat transfer is vital to turbine designers.

For a laminar free stream flow, heat transfer in the stagnation region can be predicted using Frossling's solution [1] if the pressure distribution around the object is known from say an invicid calculation. Unfortunately, in a turbine as in most other internal flows, the flow is not laminar. Combustor primary and dilution jets and the wakes from upstream blades and vanes cause high levels of turbulence. A turbulence intensity of 11% was measured at the exit of a combustor [2]; modern high enthalpy rise combustors probably produce even higher levels. Free stream turbulence can augment stagnation region heat transfer; ratios of turbulent to laminar stagnation heat transfer of 1.9 have been measured [3].

Stagnation region heat transfer augmentation in the presence of free stream turbulence is believed to be caused by vorticity amplification (see [4] for a review). Free stream turbulence can be viewed as a continuum of tangled, vortical filaments. Filaments that are convected into the stagnation region, with components normal to the stagnation line and normal to the free stream flow, are stretched and tilted by the divergence of streamlines and acceleration around the bluff body. This stretching causes the vorticity to be intensified through conservation of angular momentum. It has been shown both experimentally and numerically [5,6,7] that vorticity in the stagnation region causes heat transfer to be increased while the boundary layer remains laminar.

It has been known for many years that free stream turbulence can augment stagnation region heat transfer [8,9]; however, results of experiments are inconsistent and attempts to correlate heat transfer augmentation as a function of turbulence intensity and Reynolds number, while ignoring the length scale, [10,11,12,13,14] have not been entirely successful. Any resulting correlations usually predict the author's data but not data from other researchers.

Lowery and Vachon [15] measured lateral length scale in

their study of the effect of grid generated turbulence on stagnation region heat transfer but they did not have a sufficient variety of grids to deduce an effect of scale. Their resulting correlation has been used as a standard against which subsequent data sets have been compared, sometimes with large discrepancies; see for example [16].

There have been several attempts to isolate the effect of turbulence length scale; Yardi and Sukhatme [17] used four different grids to generate a range of length scales. The four grids were all of different geometry; i.e. two were screens and two were biplane grids, all had different rod spacing to rod diameter ratios. They showed a trend of increasing heat transfer with decreasing length scale; however, there was so much scatter in the data that their claim of ten boundary layer thicknesses for an optimum length scale is questionable.

Dyban et al [18] used perforated plates as well as a fully developed turbulent pipe flow to investigate the effect of intensity and scale on stagnation region heat transfer. Their results showed increasing augmentation with decreasing scale but they did not attempt to correlate the data based on this finding.

More recently, Ames [19] used simulated combustor segments to generate turbulence and measure its effect on heat transfer to a flat plate and a stagnation region. Ames concentrated on relatively large scale turbulence where the length scale to leading edge diameter ratio was greater than 1.0. He used the rapid distortion theory of Hunt [20] and the measurements of Hunt and Graham [21] near a plane surface to develop a new correlating parameter involving Reynolds number, turbulence intensity, and what Ames calls an energy scale (the average size of the energy containing eddies). Ames used three different diameter cylinders to investigate stagnation region heat transfer; his data were correlated well using his new parameter. The data of several other researchers were also correlated by his parameter but with more scatter.

Van Fossen and Ching [22] measured heat transfer on a circular leading edge downstream of four different square bar, square mesh turbulence generating grids. They developed a correlation for stagnation region heat transfer involving turbulence intensity, integral length scale, and Reynolds number that fit their results to ±4% and the results of other authors with similar turbulence generators to within ±8%.

Considering vorticity amplification theory, it would seem reasonable that leading edge velocity gradient would have an effect on stagnation heat transfer. Higher velocity gradients would cause more rapid stretching of the vortical filaments as they are convected past the leading edge thus increasing heat transfer. The purpose of the present work was to study the effect of leading edge velocity gradient on stagnation region heat transfer augmentation. Three models with elliptical leading edges were fabricated with heat transfer gages in the stagnation region. The ratio of major to minor axes for the models were: 1.5:1, 2.25:1 and 3:1. All three models had the same leading edge radius of curvature as the circular leading edge of Van Fossen and Ching [22]. Each of the models was qualified in a low turbulence flow by comparing stagnation heat transfer measurements with a numerical solution for laminar stagnation flow. The same four grids used in [22] were used to generate turbulence upstream of each model. The grids were square mesh, biplane grids made from square bars with different bar widths. Each of the four had identical mesh to bar width ratio.

Stagnation region heat transfer was measured with each grid at various distances upstream of each of the models. Data were taken at Reynolds numbers based on leading edge diameter ranging from 37,000 to 228,000. Turbulence intensities were in the range 1.1 to 15.9 percent while the ratio of integral length scale to leading edge diameter ranged from 0.05 to 0.30. Stagnation point velocity gradient varied from 1.20 to 1.80.

It will be shown that stagnation heat transfer augmentation due to turbulence is unaffected by the velocity gradient near the leading edge and can be predicted for each of the elliptical bodies by the same correlation developed for the circular leading edge [22]. A method for determining the heat transfer distribution downstream of the stagnation point will also be presented.

NOMENCLATURE

A	surface area of gage, m^2
a	constant in equation (9)
a_e	ellipse major axis
B	ratio of model thickness to tunnel height
b	turbulence grid bar width, cm
b_e	ellipse minor axis, cm
C	constant equation (11)
C_{hw}	constant in equation (7)
C_τ	parameter in equation (1)
d	diameter of model leading edge = $2R$, cm
E	mean hot wire voltage, V
e_{RMS}	fluctuating output voltage from linearizer, V
$Fr(s/R)$	Frossling number
I	constant in equation (10)
k	air thermal conductivity, W/mK
M	mesh spacing of bars in turbulence grid, cm
m	exponent in equation (9)
n	exponent in equation (7)
Nu	Nusselt number
Pr	Prandtl number
q	heat flow, W
R	leading edge radius, cm
Re	Reynolds number
$R(\tau)$	autocorrelation of velocity signal
r	recovery factor
s	surface distance from stagnation, cm
T	temperature, °C
Tu	turbulence intensity
U	mean velocity, m/s
u'	streamwise RMS fluctuating velocity component
x	streamwise distance, cm

Greek symbols

Λ	integral length scale, cm
ρ	air density, Kgm/m^3
σ	standard deviation
τ	time shift, s

Φ heat transfer augmentation factor, equation (12)

Subscripts

0	evaluated at zero flow
avg	average
b	bar width
d	leading edge diameter
EI	electrical heating
gap	epoxy filled gap between gages
lam	laminar free stream
r	recovery
rad	radiation
st	static
t	total
turb	turbulent free stream
w	wall
x	streamwise
∞	free stream

TEST FACILITY & INSTRUMENTATION

Wind Tunnel

The experiments were carried out in the wind tunnel shown in Fig. 1, which is described in detail by Van Fossen and Simoneau [6]. Air drawn from the test cell passes through a flow conditioning section and a 4.85:1 contraction before entering the 15.2 cm wide by 68.6 cm high test section. The maximum velocity attainable was about 46 m/sec. Clear tunnel turbulence levels were less than 0.5 percent for all flow rates. After leaving the test section, the flow passed through a transition section into a 10-inch pipe which contained a standard ASME orifice run with flange taps. Air then passed through a butterfly valve which was used to control the tunnel flow rate and then to the Laboratory exhaust system. The readings from four Chromel-Constantan thermocouples located around the perimeter of the inlet to the conditioning section were averaged to yield the stagnation temperature.

Turbulence Grids

For the present tests, four square bar, square mesh, biplane turbulence generating grids were used. The grids were fabricated keeping the ratio of mesh spacing to bar width constant at 4.5 yielding an open area of 60.5 percent. Grid parameters are defined in Fig. 2 and dimensions of the grids are given in Table I. Henceforth grids will be referred to by the symbol given in the table. Turbulence generating grids could be installed at axial locations ranging from 2.41 to 52.3 cm upstream of the model stagnation point allowing length scale and intensity to be varied.

Heat Transfer Models

The four heat transfer models used in this study had elliptical leading edges. The ratio of major to minor axes, a_e/b_e, were 1:1, 1.5:1, 2.25:1 and 3:1. All models had the same radius of curvature, R, of 3.30 cm at the stagnation point. A comparison of the model profiles is shown in Fig. 3. All models had wedge shaped afterbodies that extended about 61 cm downstream of the leading edge to eliminate vortex shedding. Fig. 4 is a photograph of the heat transfer models and afterbodies. The purpose of the 4 models was to provide different velocity gradients in the stagnation region to determine if this would have an effect on stagnation heat transfer augmentation. Leading edge velocity gradients calculated using an invicid 2-D panel code [23] are shown in Fig. 5. Velocity gradients made dimensionless by leading edge radius and free stream velocity ranged from 1.2 to 1.8.

The circular model had nineteen heat flux gages and all the elliptical models had twenty-nine heat flux gages embedded symmetrically around the stagnation line. Fig. 6 is a sketch of a typical model cross section showing the heat flux gage arrangement. Each heat flux gage consisted of an aluminum strip 6.60 cm long by 0.476 cm wide and 0.32 cm deep. A Kapton® encapsulated, foil, electric heater was fastened to the back of each aluminum strip with pressure-sensitive adhesive. The temperature of each gage was measured by a Chromel-Alumel thermocouple embedded in a groove. A guard heater behind the heat flux gage array prevented heat conduction to the interior of the model. The average gap between the aluminum strips was 0.025 cm and was filled with epoxy. The dimensionless surface distance, s/R, from the stagnation line to the center of each gage is given in Table II. The aluminum strips were maintained at a uniform constant temperature by a specially designed control circuit, (see Van Fossen et al., [24]). Steady state, spanwise-averaged heat transfer coefficients were calculated for each aluminum strip based on the power supplied to the strip and the wall-to-fluid temperature difference.

Instrumentation and Data Acquisition

Turbulence intensities, and integral length scale were measured using a standard, 5 μm, single, hot-wire oriented perpendicular to the flow direction. A spectrum analyzer computed autocorrelations which were then used to determine the length scale.

Steady-state operating conditions (temperatures, pressures, voltage and current to gages, etc.) were recorded on the Laboratory data acquisition system called ESCORT [25]. For every heat transfer data point, twenty readings of each data channel were recorded. These twenty readings were averaged to give a single value for each channel. To eliminate any offset between data channels, a reading was obtained by shorting all the inputs to ESCORT and subtracting this "zero" from each subsequent reading.

EXPERIMENTAL PROCEDURE

Turbulence Parameters

Hot wires used in the turbulence measurements were calibrated in an open air jet at the same temperature as the wind tunnel flow. Velocity calibrations used a two point, iteration method in conjunction with the analog linearizers as described in [26]. The system frequency response was estimated to be around 30 kHz with the standard square wave test. Turbulence intensity and

integral length scale were measured at several locations downstream of each of the four grids and at several tunnel velocities without the heat transfer models present.

Heat Flux Measurements

For the heat transfer measurements, all the heat flux gages were heated to temperatures of about 46°C; the average recovery temperature of the air was around 27°C giving wall to air temperature difference of approximately 19°C. This temperature difference was a compromise; large enough to keep errors in temperature difference small and small enough to minimize thermal property variations. All of the heat flux gages were maintained at the same temperature within ±0.1°C; this was accomplished by adjusting the gain of each control circuit to maintain the gage thermocouple voltage within one microvolt. Heat flux measurements were carried out with each grid installed at several axial locations from the stagnation line of the leading edge. For each grid position, tests were performed at three Reynolds numbers ranging from 37,000 to 228,000.

DATA REDUCTION

Turbulence

Turbulence intensity downstream of the grids was calculated as the ratio of the linearized root mean square (RMS) of the fluctuating component of hot wire bridge voltage to the mean voltage.

Integral length scale was determined from the autocorrelation function, $R(\tau)$, by fitting it with an exponential function using least squares

$$R(\tau) = e^{-C_\tau \tau} \tag{1}$$

Data between $0.33 \le R(\tau) \le 1.0$ were used for the curve fit. Integrating equation (1) over time delays ranging from 0 to ∞, and using Taylor's hypothesis that time delay and streamwise distance are related by the mean velocity, U, the integral length scale then becomes

$$\Lambda_x = U\int_0^\infty R(\tau)d\tau = \frac{U}{C_\tau} \tag{2}$$

This method eliminated the problem of determining the upper limit of integration for autocorrelation functions that oscillate about zero for large time delays. More details of the turbulence measurements are presented in [27].

Heat Transfer

Power from the electric heaters is removed from the aluminum strips by convection to the air, radiation to the surroundings, and conduction to the epoxy gap between the gages where it is convected to the air. The Frossling number was determined from an energy balance on each gage

$$Fr(s/R) = \frac{(q_{EI} - q_{rad} - q_{gap})d}{A(T_w - T_r)k\sqrt{Re_d}} \tag{3}$$

where q_{EI} is the heat added by the heater (voltage x current), q_{rad} is the heat lost by radiation, and q_{gap} is the heat conducted away to the epoxy gap and to the unguarded ends of the gages. A is the exposed heat transfer gage surface area, T_w is the gage temperature, T_r is the recovery temperature at the gage location, and k is the thermal conductivity of air.

An estimate of the gap loss, q_{gap}, can be obtained from an exact solution for two-dimensional heat conduction in a rectangle half the epoxy gap width wide and the aluminum gage depth deep. Two adjacent sides are assumed insulated, one side held at the constant temperature of the aluminum strip and the final side convecting to the air at the local recovery temperature. Heat conducted out the unguarded ends of the gages can be estimated from the same analysis by assuming a large gap width. Details of this analysis are given in [24].

Corrections for radiation heat loss, q_{rad}, were made assuming gray body radiation to black surroundings and an emissivity of 0.05 for the aluminum gage. Heat lost through the sides and unguarded ends of the strips was on the order of 10 percent of the total heat flow, while the radiation heat losses were on the order of 0.2 percent.

The recovery temperature was calculated from

$$T_r = T_{st,\infty} + r(T_t - T_{st,\infty}) \tag{4}$$

where $T_{st,\infty}$ is the static temperature upstream of the model and T_t is the total temperature. The recovery factor, r, was calculated as [27]

$$r = 1 - \left(\frac{\rho U(s)}{(\rho U)_\infty}\right)^2 (1 - \sqrt{Pr}) \tag{5}$$

where the mass flow ratio, $\rho U(s)/(\rho U)_\infty$ was found from a numerical solution of the flow over the model; the solution included the effects of the tunnel walls [28].

The thermal conductivity, viscosity, and Prandtl number were evaluated at the free stream total temperature from equations given in [29]. Total temperature was used to evaluate the thermal properties because in [28] a numerical study showed that, if the thermal properties were based on a reference temperature that involved the wall temperature, reversing the direction of heat flux (cooling the wall) caused an undesirable change in the Frossling number.

The Reynolds number, Re_d, was based on the diameter of the leading edge, d, and the mass-velocity averaged between the flow

area with maximum model blockage and the unblocked upstream flow area, i.e.

$$(\rho U)_{avg} = (\rho U)_{\infty} \frac{(2-B)}{2(1-B)} \qquad (6)$$

where B is the ratio of maximum model thickness to tunnel height and ranged from 0.096 for the circular leading edge to 0.293 for the 3:1 ellipse.

UNCERTAINTY ANALYSIS

Twenty samples were obtained for each steady-state measurement and averaged to minimize random errors. Standard deviations were also obtained from the twenty samples and used as an estimate of random error. Estimates of the accuracy of each measuring instrument were then made, added to the random component, and combined by the method of Kline & McClintock [30]. Results of the uncertainty analysis indicated an average uncertainty of ±6.5% for the Frossling number. The contributions from individual measurements to the overall uncertainty in the Frossling number are shown in Fig. 7.

Error in turbulence intensity was estimated by assuming that the linearizer approximates King's law; i.e. the velocity could be expressed in terms of bridge voltage as

$$U = \left(\frac{E^2 - E_0^2}{C_{hw}} \right)^n \qquad (7)$$

where E is the bridge output voltage, E_0 is the voltage at zero velocity, and n and C_{hw} are constants. Differentiating this expression and dividing by the velocity, one obtains an expression for turbulence intensity

$$Tu = \frac{u'}{U} \approx \frac{dU}{U} = \frac{2nEe_{rms}}{E^2 - E_0^2} \qquad (8)$$

where dU is taken as the RMS of the fluctuating component of velocity, u', and dE has been replaced by the RMS of the fluctuating component of bridge voltage, e_{RMS}. The exponent, n, was assumed to be near 2.0 with an error of ±10%. The method of error estimation described above was then applied to this expression; typical uncertainties estimated for the turbulence intensity measurements were on the order of ±15%. Uncertainties of the turbulence length scale were assumed to be the same order as the turbulence intensity.

RESULTS AND DISCUSSION

Turbulence

Turbulence intensity was measured as a function of distance downstream of each grid without the heat transfer model in place. The data was in general agreement with that of Baines and Peterson [31]. Each grid and Reynolds number had slightly different characteristics so intensity data for each case were fit with a power law curve of the form

$$Tu = a \left(\frac{x}{b} \right)^m \qquad (9)$$

Coefficients for each of the curve fits appear in Table III. Turbulence intensity was found to vary by less than 5% in the spanwise direction.

In [22], X-wire measurements are reported that showed the turbulence from the square bar, square mesh grids to be nearly isotropic for x/b greater than about 25. With a few exceptions for grid G1, all the heat transfer data was obtained with the models greater than 25 bar widths downstream of the grids.

Roach [32] developed a correlation for the integral length scale of grid generated turbulence of the form

$$\frac{\Lambda_x}{b} = I \sqrt{\left(\frac{x}{b} \right)} \qquad (10)$$

Length scale data from the present grids were found to have the same square root of distance dependence but the coefficient, I, varied from grid to grid and was an average of 35% larger than the value found by Roach. The coefficients for the length scale correlation are also found in Table III.

When the model is present downstream of the grid, turbulence is distorted as the stagnation point is approached. The fluctuating component of velocity increases and the mean velocity approaches zero [6] sending intensity levels very high. This brings up the problem of where to evaluate the turbulence intensity and length scale for use in a heat transfer correlation. It was felt that tests of most turbulence producing components, e.g. combustor, would be conducted without the model present; therefore, turbulence intensity and length scale used in the following correlations were evaluated from the curve fits in Table III using the distance from the grid to the stagnation point of the model. Turbulence intensity varied from 1.1 to 15.9%. The ratio of length scale to leading edge diameter ranged from 0.05 to 0.30.

Heat Transfer

Verification. Heat transfer results in the leading edge region with no turbulence grid in the tunnel are shown in Fig. 8 for the four different models. Measured freestream turbulence intensity in this case was less than 0.5 percent. The ordinate for the heat transfer plots is the Frossling number, $Nu_d/(Re_d)^{1/2}$. Data are presented as a function of surface distance from stagnation made dimensionless by the leading edge radius, R. In all cases the data

agree, to within the estimated experimental error, with the Frossling solution obtained using velocities calculated from a panel code [23] and with a 2-dimensional numerical solution from the PARC-2D code [28] thus confirming the accuracy of the experimental technique. The worst agreement between the experimental and numerical results is for the 2.25:1 model, where the experimental results are from 1.4 to 9.2% above the numerical results at the stagnation point. The upper limit of discrepancy is above the estimated experimental error. This model seemed to have a mind of its own; some days the model gave results that agreed quite well with the numerical results and other days large errors were observed. Possible causes of this error were investigated including model profile, surface irregularities, thermocouple calibration, and clear tunnel turbulence level. The model was X-rayed to see if the internal guard heater was touching the surface heat flux gages. No obvious cause could be found; therefore, the data for this model is presented "as is".

Stagnation Point Augmentation. In [22], the stagnation heat transfer data for the circular leading edge was correlated by the function

$$Fr(0) = 0.00799 \sqrt{Tu\ Re_d^{0.800} \left(\frac{\Lambda_x}{d}\right)^{-0.574}} + C \qquad (11)$$

The constant, C, was set to the zero turbulence Frossling number of 0.939 which was determined from the PARC-2D calculation. The other constants were determined from a least square fit of the data. The function was found to correlate the data to within ±4%.

In [28], it was shown by numerical calculation that the stagnation point Frossling number with simulated turbulence (sinusoidal velocity variation upstream of the leading edge) divided by the laminar Frossling number was independent of body shape. Following this line, the correlation for the circular leading edge was modified by dividing by the laminar stagnation Frossling number. The modified correlation then gives the stagnation point heat transfer augmentation factor, Φ, due to free stream turbulence

$$\Phi = \frac{Fr(0)_{turb}}{Fr(0)_{lam}} = 0.00851 \sqrt{Tu\ Re_d^{0.800} \left(\frac{\Lambda_x}{d}\right)^{-0.574}} + 1 \qquad (12)$$

Values for the terms $Fr(0)_{lam}$ for the four models are 0.939, 0.870, 0.811, 0.775 in order from the circular leading edge (1:1 ellipse) to the 3:1 ellipse; these values were also taken from the PARC-2D numerical solutions.

Comparison of the correlation for stagnation heat transfer augmentation by free stream turbulence (equation (12)) and the experimental data is shown in Fig. 9. The correlation was developed using only the circular leading edge data, thus, the fit for that data is the best. In general, the fit is excellent falling mostly within the ±4% bands drawn on the figure. The 2.25:1 model has the most scatter; as mentioned earlier, this model had problems. If the Frossling number for the 2.25:1 model had been normalized using the average of the experimental low turbulence data instead of the numerical solution, agreement with equation (12) would have been much better. The excellent agreement for the other three models confirms the validity of this correlation method.

Equation (12) contains no term that involves the velocity gradient at the stagnation point; yet the stagnation point heat transfer augmentation is the same for several different levels of velocity gradient. Thus, the hypothesis that heat transfer augmentation above laminar levels should increase in the presence of higher velocity gradients is not born out by these experiments.

Distribution of Heat Transfer Around Leading Edge. Fig. 10 is a plot of the local Frossling number normalized by the stagnation value versus dimensionless surface distance from the stagnation point for each of the models. The symbols represent an average of the local Frossling number data for all turbulent free stream conditions (all grids, Reynolds numbers, and grid positions). The dotted lines represent the standard deviation of the normalized data and the solid line is the PARC-2D solution for a laminar free stream which has been similarly normalized. Agreement between the normalized turbulent heat transfer distribution and the normalized laminar distribution is good; thus, a good prediction of the heat transfer at a given distance from the stagnation point can be obtained by using the correlation developed to predict the stagnation heat transfer and multiplying by the ratio of local to stagnation heat transfer from a solution for the laminar free stream.

CONCLUSIONS

Spanwise average stagnation region heat transfer measurements have been made on four models with elliptical leading edges downstream of turbulence generating grids. The ratio of major to minor axes for the elliptical leading edges ranged from 1:1 to 3:1; all the models had the same leading edge radius of curvature. Velocity gradients at the stagnation point ranged from 1.20 to 1.80. Four turbulence generators were used, they were square mesh, square bar, biplane grids with identical mesh spacing to bar width ratios and bar widths ranging from 0.16 to 1.27 cm. Reynolds numbers based on leading edge diameter ranged from 37,000 to 228,000, turbulence intensities ranged from 1.1 to 15.9%, and the ratio of integral length scale to leading edge diameter ranged from 0.05 to 0.30. Results are summarized as follows:

1. The Frossling and PARC-2D solution and the experimental stagnation region heat transfer data for a laminar free stream are in good agreement for all models tested.

2. Stagnation point heat transfer augmentation by free stream turbulence for the elliptical leading edges can be predicted using

a normalized version of a previously developed correlation for a circular leading edge.

3. Dimensionless heat transfer augmentation due to turbulence is independent of body shape and therefore independent of velocity gradient at the stagnation point.

4. The heat transfer distribution downstream from the stagnation point can be predicted using the normalized laminar heat transfer distribution and the stagnation point heat transfer correlation.

REFERENCES

1. Frossling, N., "Evaporation, Heat Transfer, and Velocity Distribution in Two-Dimensional and Rotationally Symmetric Laminar Boundary-Layer Flow," NACA TN-1432, 1958

2. Zimmerman, D.R., "Laser Anemometer Measurements at the Exit of a T63-C20 Combustor," NASA CR-159623, 1979

3. Yeh, F.C., Hippensteele, S.A., Van Fossen, G.J., and Poinsatte, P.E., "High Reynolds Number and Turbulence Effects on Aerodynamics and Heat Transfer in a Turbine Cascade," presented at the AIAA/SAE/ASME/ASEE 29th Joint Propulsion Conference and Exhibit, Monterey, CA, 1993; also NASA TM-106187

4. Morkovin, M.V., "On the Question of Instabilities Upstream of Cylindrical Bodies," NASA CR-3231, 1979

5. Hanarp, L.R. and Suden, B.A., "Structure of the Boundary Layers on a Circular Cylinder in the Presence of Free Stream Turbulence," *Letters in Heat and Mass Transfer*, Vol. 9, 1982, pp. 169-177.

6. Van Fossen, G.J. and Simoneau, R.J., "A Study of the Relationship Between Free-Stream Turbulence and Stagnation Region Heat Transfer," *J. of Heat Transfer*, Vol. 109, 1987, pp. 10-15.

7. Rigby, D.L., and Van Fossen, G.J., "Increased Heat Transfer to a Cylindrical Leading Edge due to Spanwise Variations in the Freestream Velocity," presented at the AIAA 22nd Fluid Dynamics, Plasma Dynamics & Lasers Conf., Honolulu, HA, June 24-26, 1991.

8. Giedt, W.H., "Effect of Turbulence Level of Incident Air Stream on Local Heat Transfer From Cylinders," *J. of the Aeronautical Sciences*, Vol. 18, No. 11, 1951, pp. 725-730.

9. Seban, R.A., "The Influence of Free Stream Turbulence on the Local Heat Transfer From Cylinders," *J. of Heat Transfer*, Vol. 82c, 1960, pp. 101-107.

10. Zapp, G.M., "The Effect of Turbulence on Local Heat Transfer Coefficient Around a Cylinder Normal to an Air Stream," M.S. Thesis, Oregon State College, June 1950.

11. Schnautz, J.A., "Effect of Turbulence Intensity on Mass Transfer from Plates, Cylinders, and Spheres in Air Streams," PhD Thesis, Oregon State College, June 1958.

12. Smith, M.C. and Kuethe, A.M., "Effects of Turbulence on Laminar Skin Friction and Heat Transfer," *The Physics of Fluids*, Vol. 9, No. 12, 1966, pp.2337-2344.

13. Kestin, J. and Wood, R.T., "The Influence of Turbulence on Mass Transfer From Cylinders," *Trans. of the ASME, J. of Heat Transfer*, Vol. 93c, 1971, pp. 321-327.

14. Mehendale, A.B., Han, J.C., and Ou, S., "Influence of High Mainstream Turbulence on Leading Edge Heat Transfer," *J. of Heat Transfer*, Vol. 113, 1991, pp. 843-850.

15. Lowery, G.W. and Vachon, R.I., "Effect of Turbulence on Heat Transfer From Heated Cylinders," *International J. of Heat and Mass Transfer*, Vol. 18, No. 11, 1975, pp. 1229-1242.

16. O'Brien, J.E. and Van Fossen, G.J., "The Influence of Jet-Grid Turbulence on Heat Transfer from the Stagnation Region of a Cylinder in Crossflow," presented at the ASME National Heat Transfer Conference, Denver, CO, Aug. 4-7, 1985; also NASA TM-87011.

17. Yardi, N.R. and Sukhatme, S.P., "Effects of Turbulence Intensity and Integral Length Scale of a Turbulent Free Stream on Forced Convection Heat Transfer From a Circular Cylinder in Cross Flow," *Proc. of the 6th Int. Heat Transfer Conf.*, paper no. FC(b)-29, 1978, pp. 347-352.

18. Dyban, YE.P., Epic, E.YA., and Kozlova, L.G., "Heat Transfer in the Vicinity of the Front Stagnation Point of a Cylinder in Transverse Flow," *HEAT TRANSFER - Soviet Research*, Vol. 7, No. 2, 1975, pp.70-73.

19. Ames, F.E., "Heat Transfer with High Intensity, Large Scale Turbulence: The Flat Plate Turbulent Boundary Layer and the Cylindrical Stagnation Point," PhD Thesis, Stanford Univ., 1990.

20. Hunt, J.C.R., "A Theory of Turbulent Flow Round Two-Dimensional Bluff Bodies," *J. of Fluid Mechanics*, Vol. 61, Part 4, 1973, pp. 625-706.

21. Hunt, J.C.R. and Graham, J.M.R., "Free-Stream Turbulence Near Plane Boundaries," *J. of Fluid Mechanics*, Vol 84, 1978, pp. 209-235.

22. Van Fossen, G.J. and Ching, C.Y., "Measurements of the Influence of Integral Length Scale on Stagnation Region Heat Transfer," presented at the Fifth Int. Symposium on Transport Phenomena and Dynamics of Rotating Machinery, Kaanapali, Maui, HA, May 8-12, 1994, paper no. TP-16.

23. McFarland, E.R., "A FORTRAN Computer Code for Calculating Flows in Multiple-Blade-Element Cascades," NASA TM-87104, 1985.

24. Van Fossen, G.J., Simoneau, R.J., Olsen, W.A., Jr., and Shaw, R.J., "Heat Transfer Distributions Around Nominal Ice Accretion Shapes Formed on a Cylinder in the NASA Lewis Icing Research Tunnel," presented at the AIAA 22nd Aerospace Sciences Meeting, Jan. 9-12, 1984, Reno, NV, paper no. AIAA-84-0017, also NASA TM-83557.

25. Miller, R.L., "ESCORT: A Data Acquisition and Display System to Support Research Testing," NASA TM-78909, 1978.

26. Anon., *DISA Type 55M25 Linearizer Instruction Manual*, Published by DISA Information Dept. page 7, example 1.

27. Van Fossen, G.J., Simoneau, R.J., and Ching, C.Y., "The Influence of Turbulence Parameters and Velocity Gradient on Stagnation Region Heat Transfer," NASA TP to be published.

28. Rigby, D.L. and Van Fossen, G.J., "Increased Heat Transfer to Elliptical Leading Edges due to Variations in the Freestream Momentum: Numerical and Experimental Results," presented at the AIAA/SAE/ASME/ASEE 28th Joint Propulsion Conf. and Exhibit, July 6-8, 1992, Nashville, TN, AIAA paper no. AIAA-92-3070.

29. Hillsenrath, J., Beckett, C.W., Benedict, W.S., Fano, L., and Hobe, H.J., "Tables of Thermal Properties of Gases," NBS Circular 564, Nov. 1955.

30. Kline, S.J., and McClintock, F.A., "Describing Uncertainties in Single-Sample Experiments," *Mechanical Engineering*, Vol. 75, 1953, pp. 3-8.

31. Baines, W.D. and Peterson, E.G., "An Investigation of Flow Through Screens," *Trans. of the ASME*, Vol. 72, 1951, pp. 468-480.

32. Roach, P.E., "The Generation of Nearly Isotropic Turbulence by Means of Grids," *Int. J. of Heat and Fluid Flow*, Vol. 8, No. 2, 1987, pp. 89-92.

Table I. Turbulence generating grid dimensions.

GRID NO.	b, cm (in)	M/b	% OPEN AREA
G1	1.270(.500)	4.5	60.5
G2	0.635(.250)	4.5	60.5
G3	0.318(.125)	4.5	60.5
G4	0.159(.063)	4.5	60.5

Table II. Heat flux gage dimensionless surface distances from stagnation point.

MODEL	1:1	1.5:1	2.25:1	3:1
GAGE	s/R			
1	0.000	0.000	0.000	0.000
2	0.152	0.151	0.152	0.151
3	0.303	0.303	0.304	0.301
4	0.455	0.456	0.457	0.452
5	0.607	0.607	0.610	0.604
6	0.759	0.759	0.762	0.755
7	0.910	0.910	0.915	0.907
8	1.062	1.062	1.068	1.058
9	1.214	1.214	1.221	1.210
10	1.365	1.366	1.374	1.361
11		1.518	1.527	1.512
12		1.670	1.680	1.664
13		1.822	1.833	1.816
14		1.975	1.986	1.968
15		2.127	2.140	2.119

Table III. Power law curve fits of turbulence intensity and integral length scale data.

$$Tu = a\left(\frac{x}{b}\right)^{m} \qquad \frac{\Lambda_x}{b} = I\sqrt{\left(\frac{x}{b}\right)}$$

Grid	Velocity symbol	Re_b	a	m	I
G1	R1	38650	206.1	-0.875	0.240
G1	R2	18000	206.1	-0.875	0.240
G1	R3	7934	206.1	-0.875	0.240
G2	R1	17190	146.3	-0.780	0.272
G2	R2	9514	135.3	-0.758	0.272
G2	R3	4452	138.9	-0.778	0.272
G3	R1	8935	132.2	-0.765	0.264
G3	R2	4780	156.3	-0.824	0.264
G3	R3	2470	149.4	-0.830	0.264
G4	R1	4571	80.15	-0.665	0.303
G4	R2	2297	89.46	-0.693	0.303
G4	R3	1174	75.05	-0.677	0.303

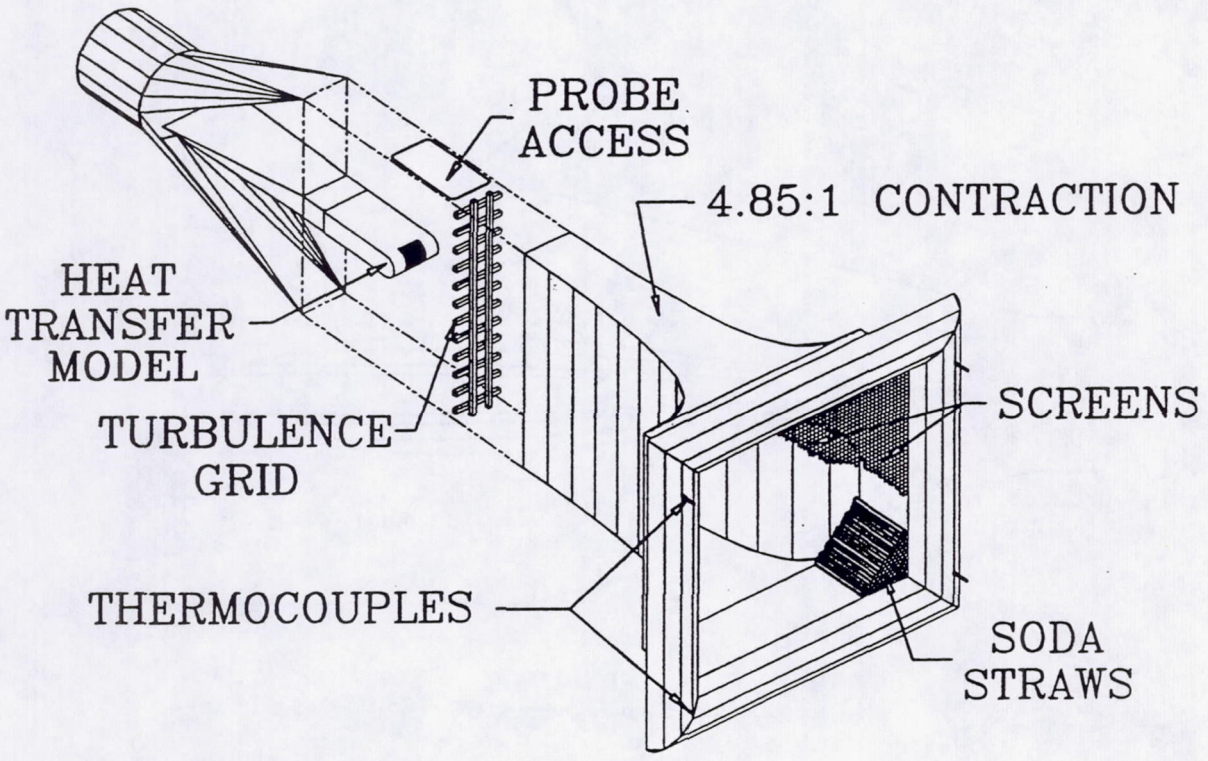

Fig. 1. Wind tunnel.

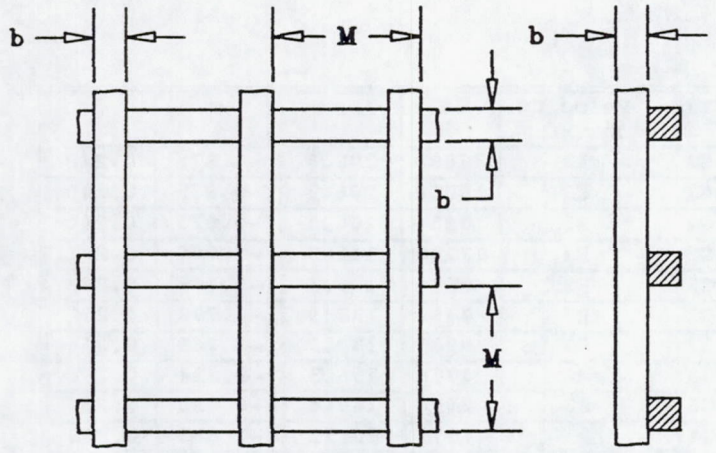

Fig. 2. Biplane grid configuration.

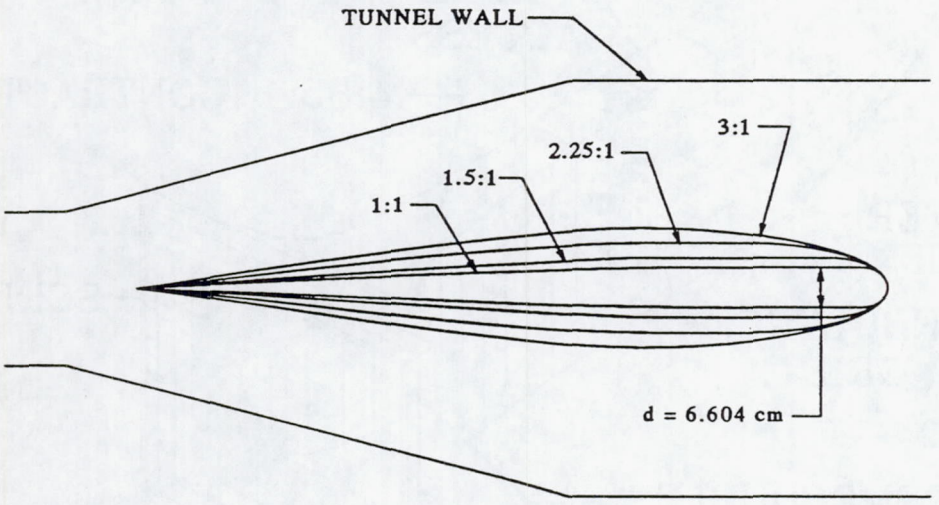

Fig. 3. Model profile comparison.

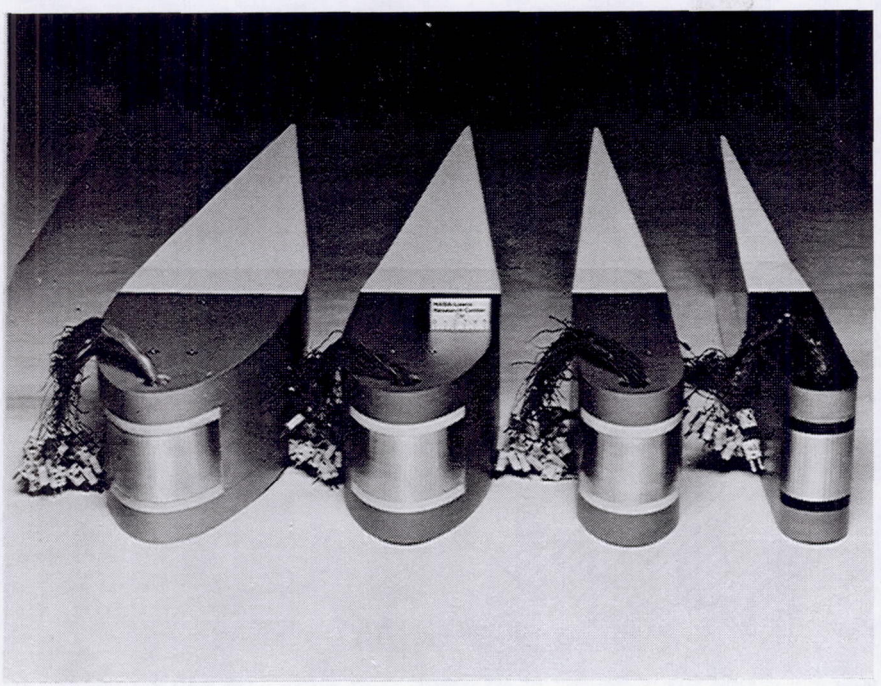

Figure 4. Elliptical leading edge models.

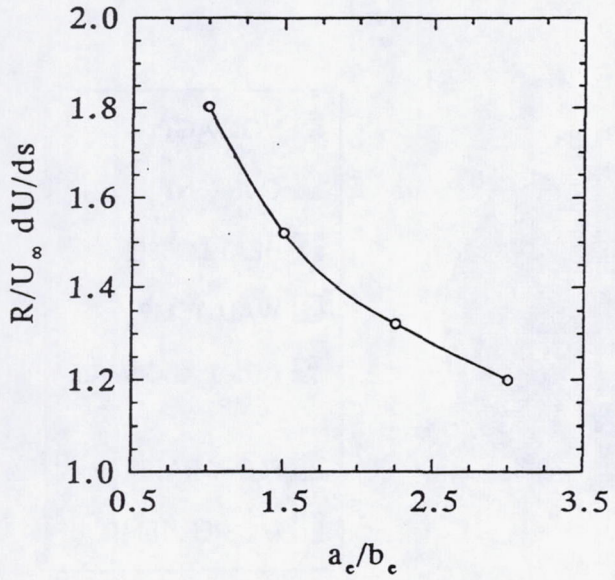

Fig. 5. Stagnation point streamwise velocity gradient versus major to minor axis ratio.

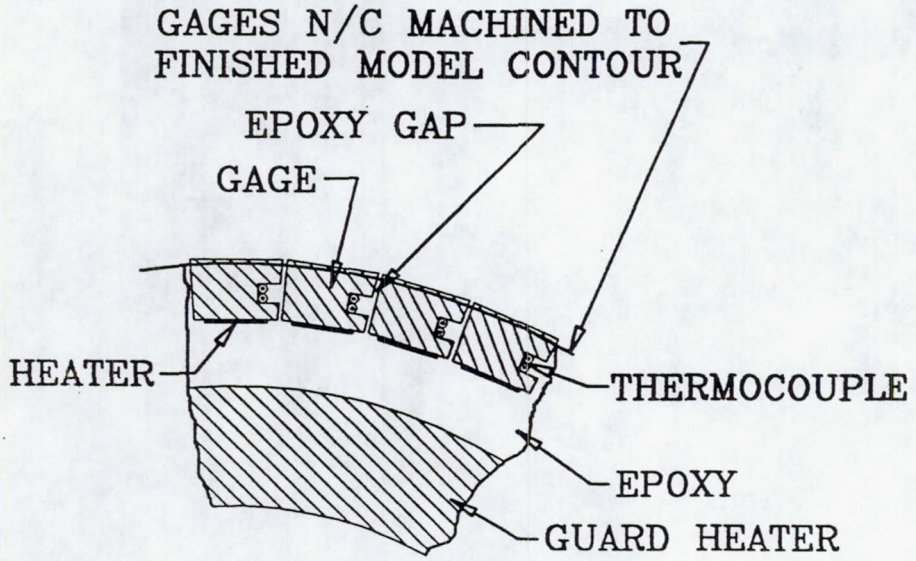

Fig. 6. Heat flux gage configuration.

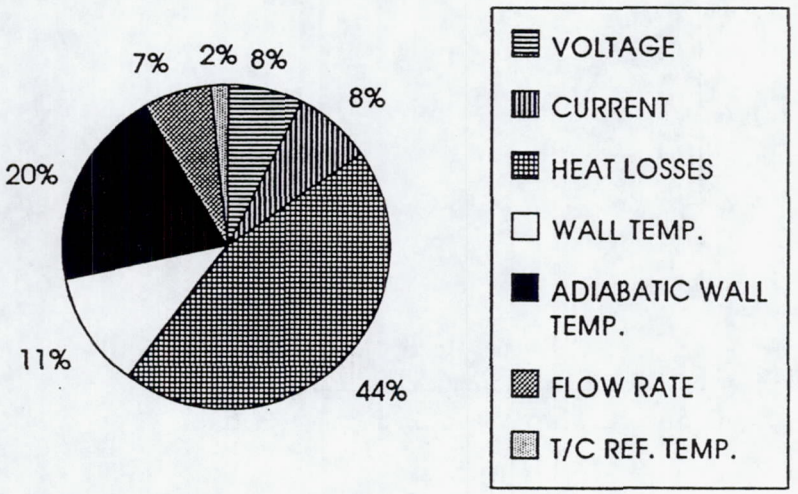

Fig. 7. Components of total uncertainty in measured Frossling number.

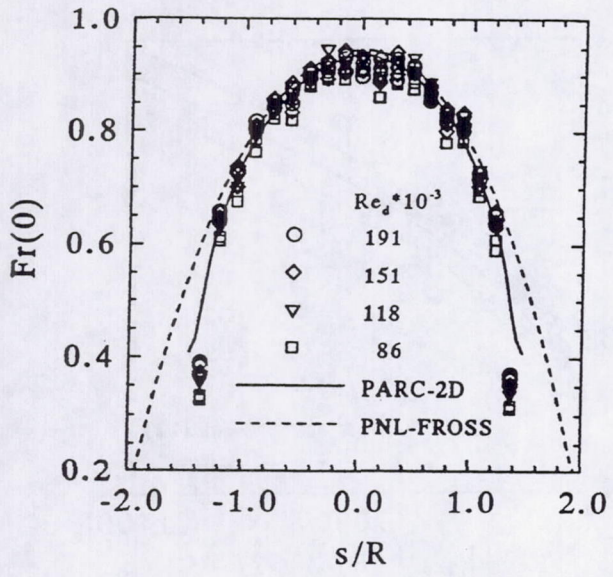

a.) 1:1 ellipse

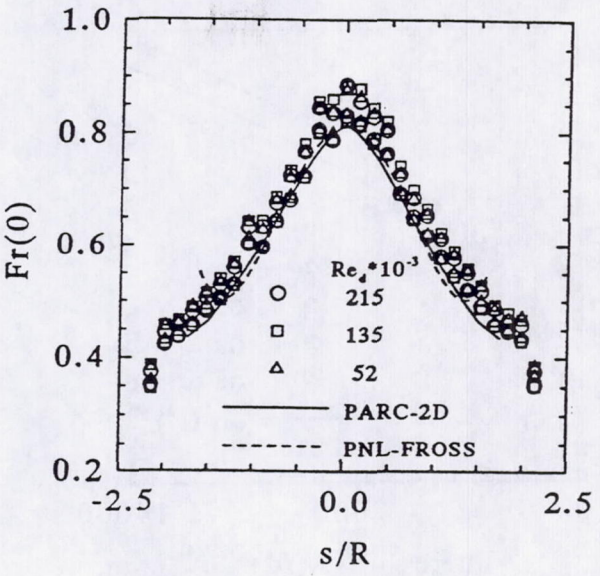

c.) 2.25:1 ellipse

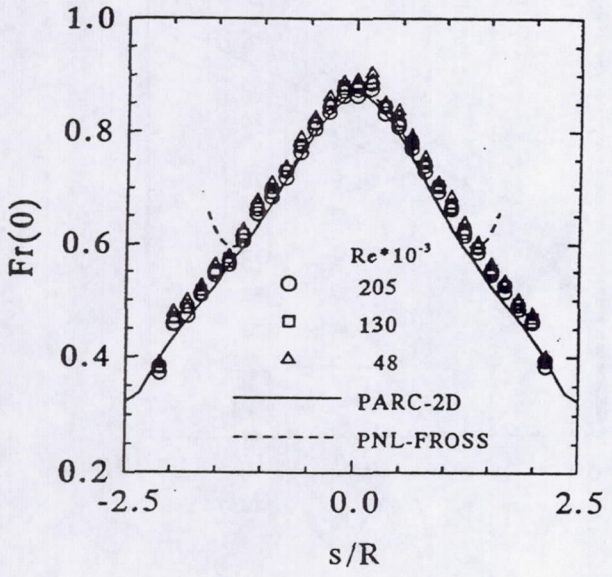

b.) 1.5:1 ellipse

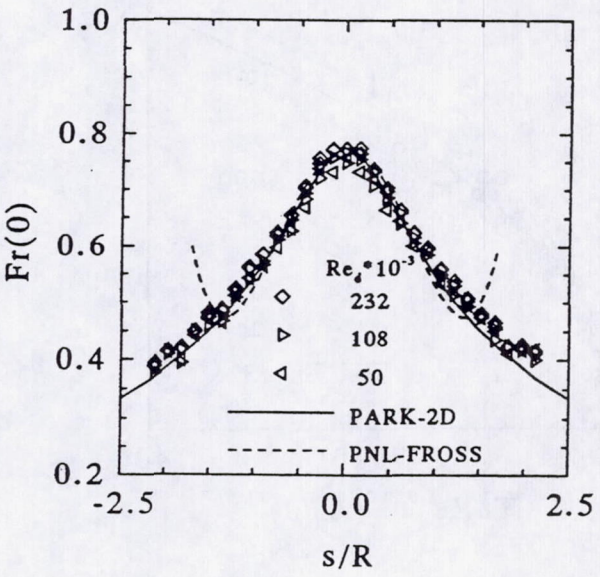

d.) 3:1 ellipse

Fig. 8. Low turbulence Frossling number distribution around leading edge compared to PARC-2D and Frossling solutions.

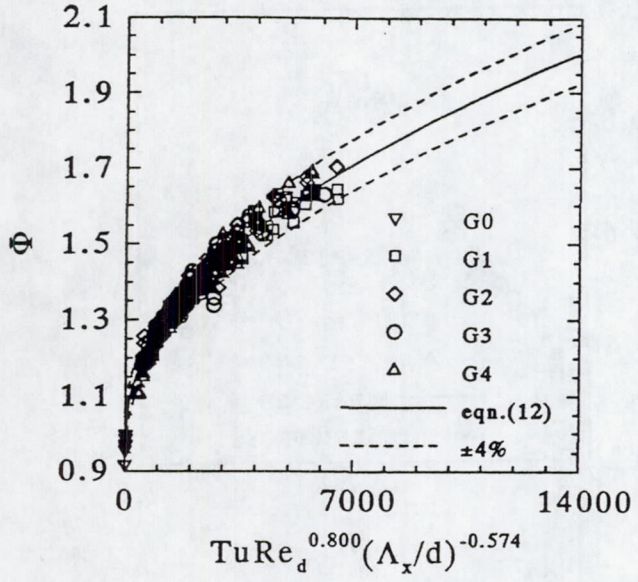

a.) 1:1 ellipse

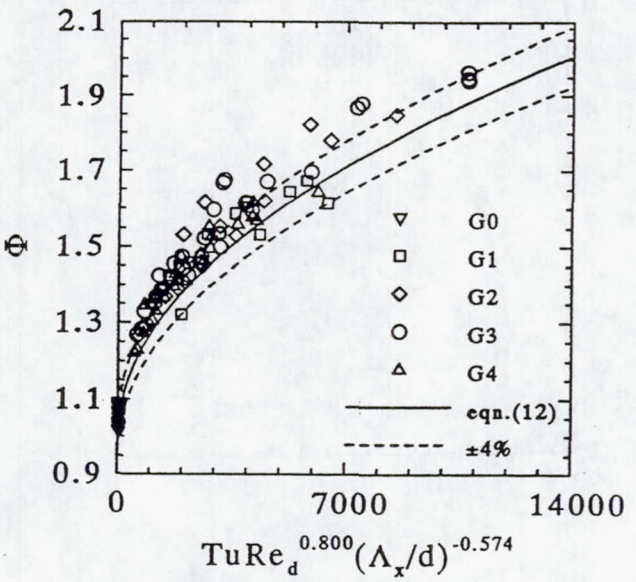

c.) 2.25:1 ellipse

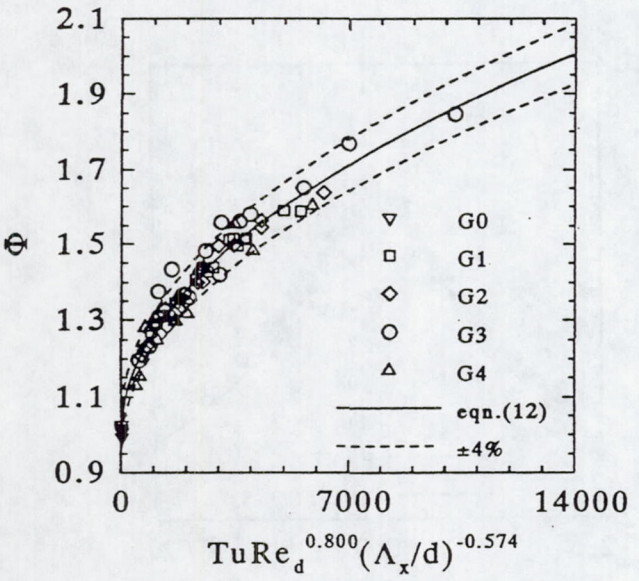

b.) 1.5:1 ellipse

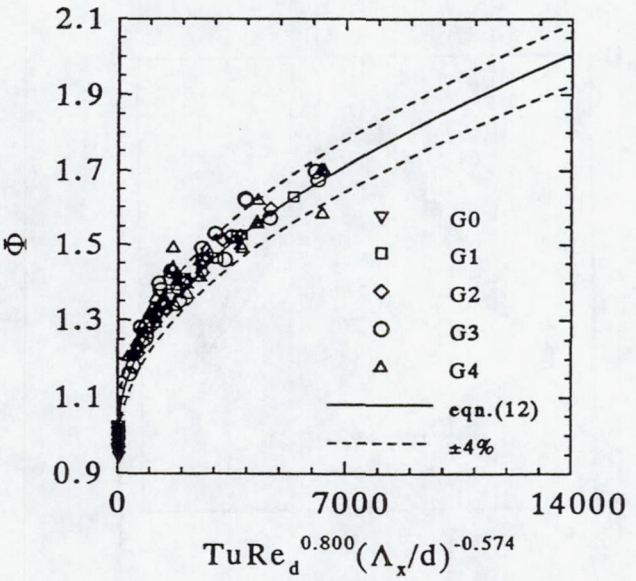

d.) 3:1 ellipse

Fig. 9. Comparison of stagnation point heat transfer augmentation data and correlation.

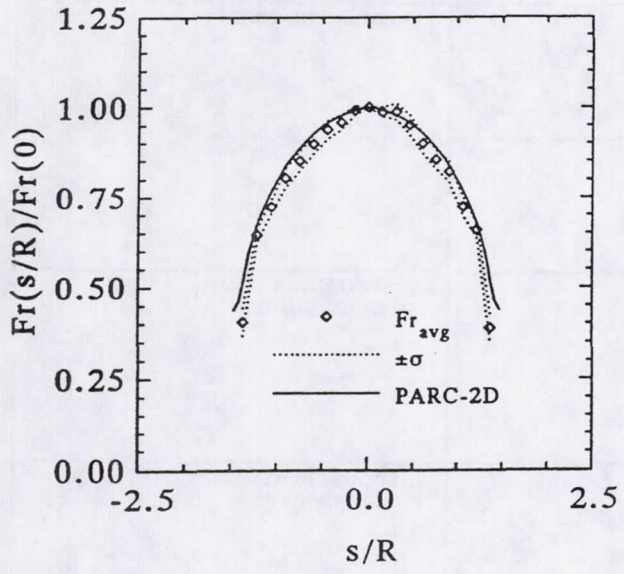

a.) 1:1 ellipse

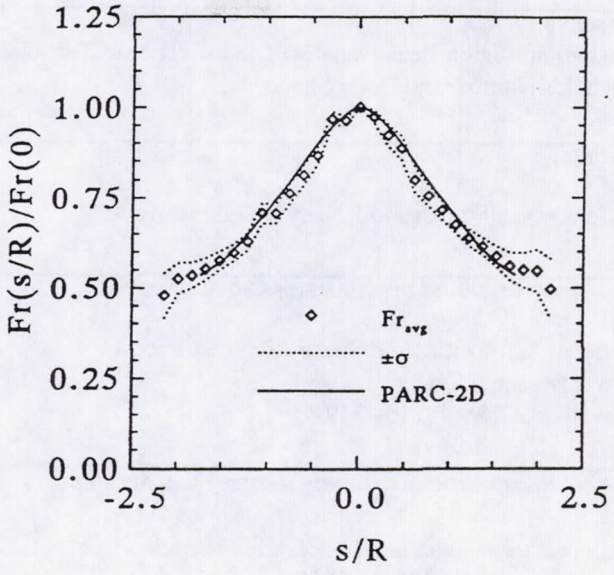

c.) 2.25:1 ellipse

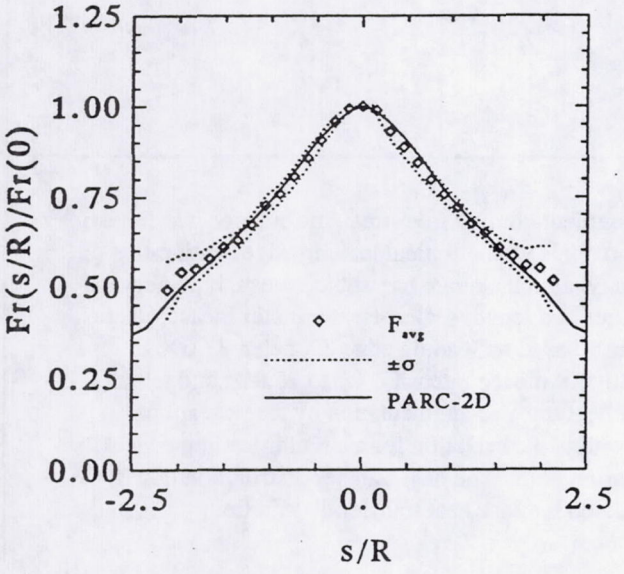

b.) 1.5:1 ellipse

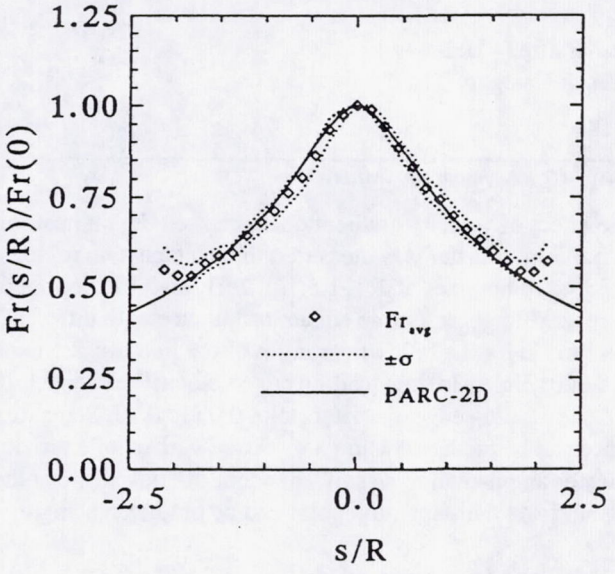

d.) 3:1 ellipse

Fig. 10. Distribution of averaged, normalized Frossling number downstream of stagnation point.

REPORT DOCUMENTATION PAGE

Form Approved
OMB No. 0704-0188

1. AGENCY USE ONLY (*Leave blank*)	2. REPORT DATE	3. REPORT TYPE AND DATES COVERED
	February 1994	Technical Memorandum

4. TITLE AND SUBTITLE

Stagnation Region Heat Transfer: The Influence of Turbulence Parameters, Reynolds Number and Body Shape

5. FUNDING NUMBERS

WU–505–62–52

6. AUTHOR(S)

G. James Van Fossen and Robert J. Simoneau

7. PERFORMING ORGANIZATION NAME(S) AND ADDRESS(ES)

National Aeronautics and Space Administration
Lewis Research Center
Cleveland, Ohio 44135–3191

8. PERFORMING ORGANIZATION REPORT NUMBER

E–8534

9. SPONSORING/MONITORING AGENCY NAME(S) AND ADDRESS(ES)

National Aeronautics and Space Administration
Washington, D.C. 20546–0001

10. SPONSORING/MONITORING AGENCY REPORT NUMBER

NASA TM–106504

11. SUPPLEMENTARY NOTES

Prepared for the Sixth AIAA/ASME Thermophysics and Heat Transfer Conference cosponsored by the American Institute of Aeronautics and Astronautics and the American Society of Mechanical Engineers, Colorado Springs, Colorado, June 20–23, 1994. Responsible person, G. James Van Fossen, organization code 2630, (216) 433–5892.

12a. DISTRIBUTION/AVAILABILITY STATEMENT

Unclassified - Unlimited
Subject Category 34

12b. DISTRIBUTION CODE

13. ABSTRACT ***(Maximum 200 words)***

The effect of velocity gradient on stagnation region heat transfer augmentation by free stream turbulence was investigated. Heat transfer was measured in the stagnation region of four models with elliptical leading edges with ratios of major to minor axes of 1:1, 1.5:1, 2.25:1, and 3:1. Four geometrically similar, square bar, square mesh, biplane grids were used to generate free stream turbulence with different intensities and length scales. Heat transfer measurements were made for the following ranges of parameters: Reynolds number, based on leading edge diameter, 37,000 to 228,000; dimensionless leading edge velocity gradient, 1.20 to 1.80; turbulence intensity, 1.1 to 15.9%; and length scale to leading edge diameter ratio, 0.05 to 0.30. Stagnation point heat transfer augmentation by free stream turbulence can be predicted using a modified version of a previously developed correlation for a circular leading edge. Heat transfer augmentation was independent of body shape at the stagnation point. The heat transfer distribution downstream from the stagnation point can be predicted using the normalized laminar heat transfer distribution.

14. SUBJECT TERMS

Heat transfer; Stagnation flow; Turbulence

15. NUMBER OF PAGES

17

16. PRICE CODE

A03

17. SECURITY CLASSIFICATION OF REPORT	18. SECURITY CLASSIFICATION OF THIS PAGE	19. SECURITY CLASSIFICATION OF ABSTRACT	20. LIMITATION OF ABSTRACT
Unclassified	Unclassified	Unclassified	